Fatigue Life Prediction for Circular Rubber Bearings Subjected to Cyclic Compression

Hsoung-Wei Chou,[1] Jong-Shin Huang[2]

[1]*Institute of Nuclear Energy Research, Taoyuan 32546, Taiwan*
[2]*Department of Civil Engineering, National Cheng Kung University, Tainan 70101, Taiwan*

Received 21 February 2011; accepted 20 April 2011
DOI 10.1002/app.34732
Published online 23 August 2011 in Wiley Online Library (wileyonlinelibrary.com).

ABSTRACT: The fatigue life of circular rubber bearings under cyclic compression is theoretically and numerically analyzed based on a previously proposed fatigue failure mechanism. The energy release rate at any point in circular rubber bearings under cyclic compression, which depends on the cracking energy density and crack length along the predicted crack propagation path, is derived first theoretically. Then, the corresponding fatigue crack growth rate and fatigue life are determined numerically by introducing the fatigue parameters of three different rubber compounds before and after suffering from thermal aging. Meanwhile, the effects of intrinsic flaw size and maximum compressive stress on the fatigue life of circular rubber bearings are also investigated. It is found that the enlargement in the Regime 1 range of the crack growth rate of rubber increases the fatigue resistance of circular rubber bearings. Therefore, the effects of the mechanical properties, intrinsic flaw size, threshold value, and maximum cyclic compressive stress on fatigue life are significant and should be taken into account in designing rubber bearings. © 2011 Wiley Periodicals, Inc. J Appl Polym Sci 123: 2194–2203, 2012

Key words: fatigue; shape factor; cracking energy density; intrinsic flaw size

INTRODUCTION

Rubber bearings composed of multiple layers of rubber and steel plate are widely used as earthquake isolators in buildings and bridges. Such rubber bearings need to provide sufficient vertical stiffness to sustain the total weight of upper structures and energy absorption to protect them from a seismic damage. When rubber bearings are utilized as isolators and dampers in buildings and bridges, fatigue failure is most likely to occur due to cyclic compression. For example, overloaded vehicles passing over bridges or live loads acting on buildings are frequently observed in Taiwan. Fatigue failure of rubber bearings under cyclic compression is mainly caused by the crack initiation and propagation in rubbery materials. The degradation of circular neoprene rubber bearings resulting from fatigue failure under cyclic compression was investigated experimentally by Chou and Huang.[1] The experimental observations of saw-cut cross sections of their specimens indicates the fatigue cracks initiate at the interfaces between rubber and steel plates, and then propagate steadily in rubber, inevitably reducing the dynamic responses of rubber bearings. In some cases, the fatigue failure of rubber bearings caused by cyclic compression could lead to a catastrophic failure of buildings and bridges, even when they are subjected to earthquakes with only an intermediate intensity. Therefore, theoretical prediction of the fatigue life of rubber bearings subjected to cyclic compression needs to be undertaken in more detail when both structural integrity and durability of buildings and bridges are sought.

To evaluate the fatigue resistance of rubbery materials under a multiaxial stress state, Mars[2,3] introduced the concept of cracking energy density, defined as the work produced by the principal stresses acting directly on each existing crack. It is suggested that the energy required to tear a crack or employed to determine the direction of crack propagation in rubbery materials under multiaxial stresses is the cracking energy density. The cracking energy density, W_C, around a crack in rubbery materials under multiaxial stresses can be calculated as follows:

$$W_C = \hat{r}^T \kappa^T \left[\int_0^{\bar{\varepsilon}} \bar{\sigma} d\bar{\varepsilon} \right] \kappa \hat{r}, \tag{1}$$

where $\hat{r}$ is a unit vector normal to the crack surface plane, κ is the transformation matrix from the crack

Correspondence to: J.-S. Huang (jshuang@mail.ncku.edu.tw).

Contract grant sponsor: National Science Council, Taiwan, R.O.C.; contract grant number: NSC 91-2211-E006-113.

surface plane to the principal stress plane, and $\bar{\sigma}$ and $\bar{\varepsilon}$ are the induced principal stresses and strains acting around the crack due to external multiaxial stresses. If there are no relatively large pre-existing cracks in the rubbery materials, the orientation of the maximum cracking energy density at any point is the direction of the maximum principal tensile stress.[2] Therefore, the fatigue crack initiates from a point with maximum cracking energy density and propagates along the direction of principal stress. In evaluating the fatigue properties of rubbery materials, such as crack propagation and life prediction, the maximum principal tensile stress has been regarded as a decisive factor by many researchers.[3–6]

An energy approach is generally utilized to analyze the tear resistance of rubber. The energy release rate, G, of rubber containing a crack under a uniaxial stretch was found to be related to its strain energy density, W, tensile strain, ε, and the crack length, c[7,8]: $G = 2\pi(1 + \varepsilon)^{-1/2} W_C$. When rubber is under multiaxial stresses, Mars[2] suggested that the energy required to tear a crack is the cracking energy density, W_C, in the above expression of the energy release rate to determine their fatigue crack growth rate, dc/dn. The effects of energy release rate on the fatigue crack growth rate of rubbery materials were reported by Lake and Lindley.[9–11] Under cyclic tensile loading with a zero stress ratio, the fatigue crack growth rate of rubber with respect to various energy release rates is divided into four regimes,[12] as schematically illustrated in Figure 1. When the energy release rate is above the smallest value of G_z around 10^{-4}KJ/m^2[13] and below a threshold value, G_0, the fatigue crack growth rate, dc/dn, in Regime 1 is much slower and remains almost constant, depending on the ozone concentration in atmosphere. However, dc/dn in Regime 4 becomes infinite when G is higher than a critical value of G_c, at which fast fracturing of the rubber occurs. There is then a transition value, G_t, between the threshold value, G_0, and the critical value, G_c.

In Regime 2, the fatigue crack growth rate of rubber increases linearly first with increasing energy release rate:

$$\frac{dc}{dn} = A(G - G_0) \quad \text{for} \quad G_0 \le G \le G_t, \tag{2}$$

where A is a fatigue parameter and should be determined experimentally. The fatigue crack growth rate of the rubber in Regime 3 then increases dramatically with the increasing energy release rate. A power-law relationship with the two fatigue parameters a and b is utilized to describe the fatigue crack growth rate of rubber:

$$\frac{dc}{dn} = aG^b \quad \text{for} \quad G_t \le G \le G_c. \tag{3}$$

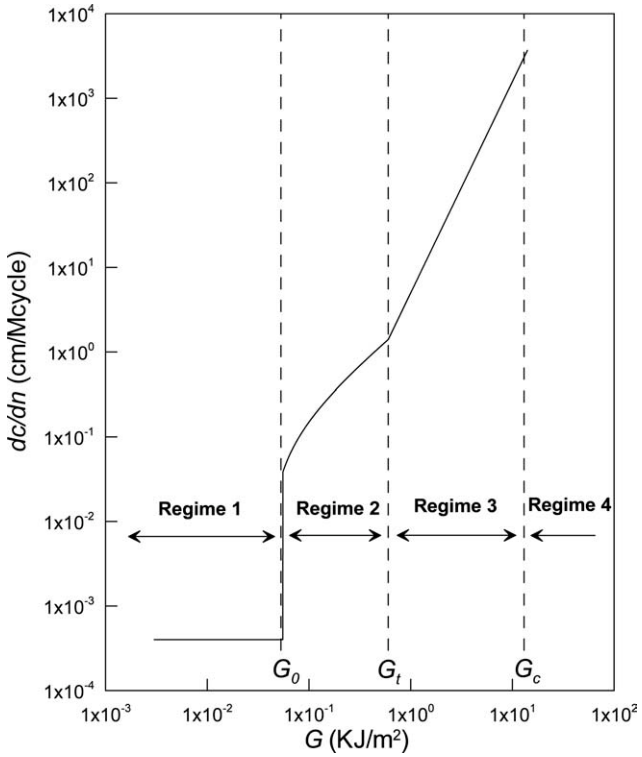

Figure 1 Four different regimes of crack growth rates of rubbers with respect to various energy release rates.

A crack in rubber is thus grown successively by cyclic extension through the above four regimes with different rates until a catastrophic rupture occurs.

On the other hand, intrinsic flaws resulting from the manufacturing process distribute randomly in rubber, and their size is another essential material parameter in estimating the fatigue life.[10,14] The intrinsic flaw size, c_0, in rubber compounds depends on carbon black type,[15] crosslink density,[16] dispersion of compound ingredients,[17] and thermal aging attack.[18] Consequently, the fatigue crack initiates at the point with maximum cracking energy density from the accumulation of intrinsic flaws in rubber, subsequently propagates along a direction perpendicular to the maximum tensile principal stress. In the paper, we aim to theoretically estimate the fatigue life of circular rubber bearings under cyclic compression, based on the results of crack initiation and propagation obtained by quasi-static analysis.[19] First, the energy release rate which depends on the cracking energy density and crack length in bonded rubber cylinders under quasi-static compression is calculated. Then, their fatigue behaviors, such as crack growth rate and fatigue life, are determined. On the basis of the fatigue parameters of three rubber compounds,[18] the effects of mechanical properties, thermal aging, intrinsic flaw size, and maximum compressive stress on the fatigue life of

circular rubber bearings are also investigated. Consequently, the fatigue lives of circular rubber bearings obtained from different circumstances are calculated and then compared with each other.

THEORETICAL ANALYSIS

It is known that the characteristics of a rubber bearing mainly depend on the mechanical properties of rubber and the shape factor, S, the ratio of compressed surface area to lateral free surface area of each bonded rubber layer. For bonded rubber cylinders, their shape factor is expressed as $S = R/2h$; here, R is the radius and h is the thickness of a rubber cylinder, as schematically illustrated in Figure 2(a). For simplicity, a perfectly bonded rubber cylinder subjected to a compressive strain ε_c can be analyzed from an axisymmetrical model plotted on the r–z plane in a cylindrical coordinate system, as shown in Figure 2(b). The theoretical expression of stress distribution derived by Horton et al.[20] is verified to be relatively accurate, and thus is utilized here to determine the principal stresses and the resulting cracking energy density at any point in a bonded rubber cylinder under compression. The

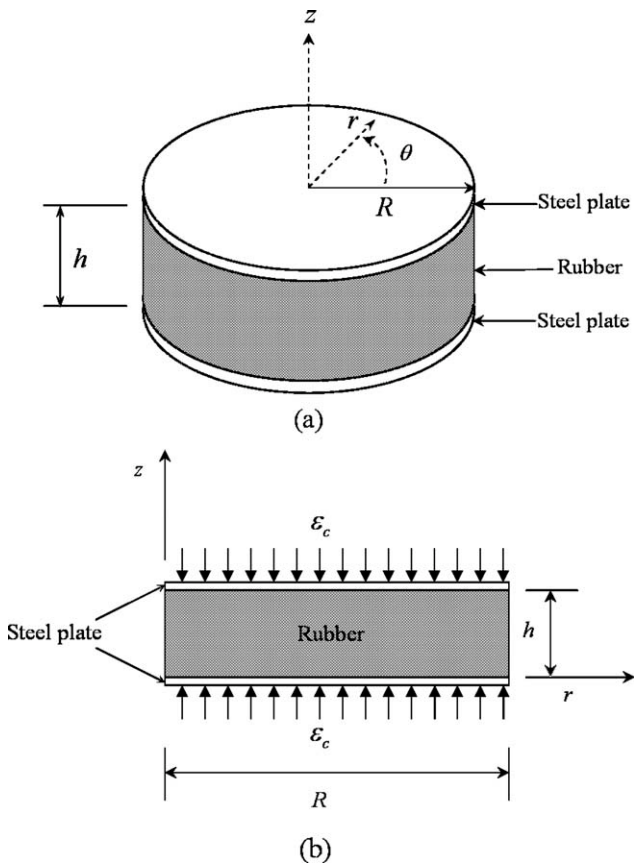

Figure 2 (a) The dimensions of a bonded rubber cylinder and (b) an axisymmetrical model on the r-z plane in a cylindrical coordinate system.

stress components in a bonded rubber cylinder obtained from Horton's method are as follows:

$$\sigma_{rr} = \sigma_{\theta\theta} = \frac{2F}{A_c}\left(1 - \frac{r^2}{R^2}\right)\frac{\cosh\left[\beta\left(z - \frac{h}{2}\right)\right]}{\cosh\frac{\beta h}{2}}, \quad (4)$$

$$\sigma_{zz} = \frac{F}{A_c}\left\{1 + \left(1 - \frac{2r^2}{R^2}\right)\frac{\cosh\left[\beta\left(z - \frac{h}{2}\right)\right]}{\cosh\frac{\beta h}{2}}\right\}, \quad (5)$$

$$\sigma_{rz} = -\frac{F\beta r}{6A_c}\frac{\sinh\left[\beta\left(z - \frac{h}{2}\right)\right]}{\cosh\frac{\beta h}{2}}, \quad (6)$$

where $\beta = \sqrt{24/R^2}$, F is the external axial force and A_c is the cross-sectional area of bonded rubber cylinders. Therefore, the principal stresses at any point in rubber, σ_{P1} and σ_{P2}, can be transformed and the resulting cracking energy density can be calculated from Eq. (1), giving:

$$W_C = \frac{1}{2E}\left(\sigma_{P1}^2 - \nu\sigma_{P1}\sigma_{P2} - \nu\sigma_{P1}\sigma_{\theta\theta}\right), \quad (7)$$

wherein, E is the Young's modulus and ν is the Poisson's ratio of rubber.

To calculate the fatigue lives of circular rubber bearings, Chou and Huang[19] proposed a fatigue failure mechanism using a quasi statically numerical methods with three assumptions. First, intrinsic flaws with a uniform size distribute randomly in rubber. In other words, no intrinsic flaws are large enough to affect the crack propagation in bonded rubber cylinders, and thus isotropy and small deformations of rubber are considered here. Second, the stress distribution in rubber still remains the same when the crack grows steadily. That is, the fatigue crack is relatively small when compared with the dimension of bonded rubber cylinders, and thus the effect of crack propagation on the stress field of bonded rubber cylinders is negligible. Thirdly, principal tensile stress dominates the crack propagation in rubber, and the orientation of crack propagation is decided by the minimum strain energy density method.[21] The fatigue crack in bonded rubber cylinders thus initiates at the point with the maximum cracking energy density, and then propagates along the direction with the lowest cracking energy density. On the basis of Horton's theory, the curves which describe the crack initiation and propagation in bonded rubber cylinders with various shape factors under cyclic compression were determined, and these were also consistent with the experimental observations and the simulations of quasi-static finite element numerical analyses.[19] It is found that the fatigue cracks initiate at the outermost boundary ($r/R = 1$) between rubber and steel plates and propagate inward to the center of circular rubber bearings. Figure 3 shows the normalized curves of crack

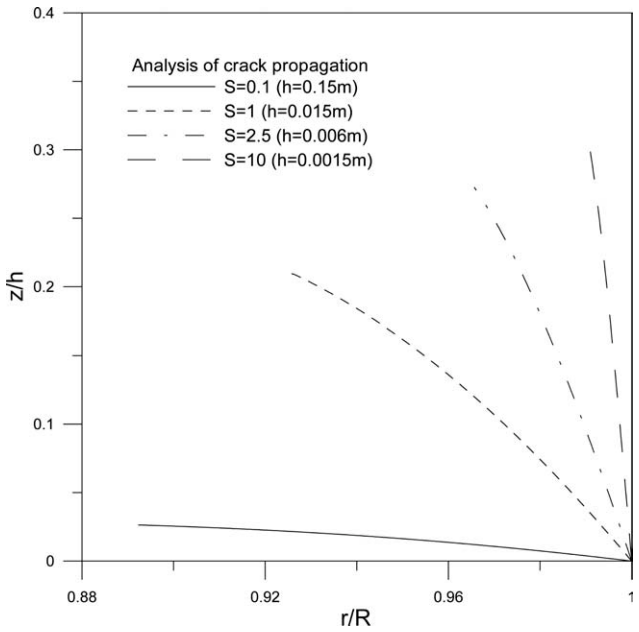

Figure 3 The normalized crack propagation paths in bonded rubber cylinders with different shape factors of $S = 0.1$, 1.0, 2.5, and 10 derived from Horton's theory.[19]

propagation in bonded rubber cylinders with different shape factors of $S = 0.1$, 1.0, 2.5, and 10, respectively, derived numerically from Horton's approach. It should be noted that no analytical solution for the curves of crack propagation can be obtained due to the complicated stress distribution in bonded rubber cylinders. Hence, a second order function, z/h, of a variable r/R is employed here to describe the crack propagation in the cylinders:

$$\frac{z}{h} = a_1\left(\frac{r}{R}\right)^2 + a_2\left(\frac{r}{R}\right) + a_3. \tag{8}$$

Herein, a_1, a_2, and a_3 are coefficients obtained from regression analysis. Table I lists the three linear regressive coefficients for bonded rubber cylinders with different shape factors. Along the curve of crack propagation, the stress components in eqs. (4)–(6) are reduced in terms of only one variable, r, as $\sigma_{rr}(r)$, $\sigma_{\theta\theta}(r)$, $\sigma_{zz}(r)$, and $\sigma_{rz}(r)$. Thus, the corresponding in-plane principal stresses and cracking energy density in Eq. (7) can eventually be regarded as $\sigma_{P1}(r)$, $\sigma_{P2}(r)$, and $W_C(r)$.

When a crack propagates gradually in a bonded rubber cylinder under cyclic compression, its length, c, is determined as the length of the curve of Eq. (8), giving:

$$\begin{aligned} c(r) &= -\int \sqrt{1 + [z'(r)]^2}\,dr + C_1 \\ &= -\int \sqrt{1 + \left(\frac{2a_1h}{a^2}r + \frac{a_2h}{a}\right)^2}\,dr + C_1. \end{aligned} \tag{9}$$

The constant C_1 can be determined by imposing the boundary condition of $c = 0$ at $r = R$ in Eq. (9). The negative sign in Eq. (9) represents an inverse direction of the integration, corresponding to the direction of crack propagation. Thus, rearranging Eq. (9) gives as follows:

$$\begin{aligned} c(r) = -\Bigg[&\frac{(2K_1r + K_2)}{4K_1}\sqrt{K_1r^2 + K_2r + K_3} \\ &+ \frac{1}{2\sqrt{K_1}}\log\left(\frac{K_2/2 + K_1r}{\sqrt{K_1}} + \sqrt{K_1r^2 + K_2r + K_3}\right)K_3 \\ &- \frac{1}{8K_1^{3/2}}\log\left(\frac{K_2/2 + K_1r}{\sqrt{K_1}} + \sqrt{K_1r^2 + K_2r + K_3}\right)K_2^2\Bigg] + C_1, \end{aligned} \tag{10}$$

where, $K_1 = (2a_1h/R^2)^2$, $K_2 = 4a_1a_2h^2/R^3$, and $K_3 = (a_2h/R)^2 + 1$, respectively. Therefore, the energy release rate, $G(r) = 2\pi[1 + \varepsilon_{P1}(r)]^{-1/2}W_C(r)c(r)$, can be obtained and the corresponding crack growth rate, dc/dn, and the fatigue cycle, n, of a circular rubber bearing under cyclic compression are determined.

Assuming the fatigue failure initiates from an intrinsic flaw with a length of its size, c_0, then the initial energy release rate is obtained by prescribing the coordinate r corresponding to $c(r) = c_0$. The energy release rate then increases gradually as the crack grows steadily. If the initial energy release rate is found to be in Regime 1, namely $G \le G_0$, the crack growth rate, dc/dn, remains constant. Hence, the fatigue cycle between Regime 1 is as follows:

$$n = \int_{c_0}^{c_{G_0}} \frac{dc}{\gamma} = \frac{c_{G_0} - c_0}{\gamma}. \tag{11}$$

Here, c_{G_0} denotes the crack length which corresponds to the case of $G = G_0$ and γ is the crack growth rate of rubber in Regime 1. When the crack advances steadily until the energy release rate, G, exceeds G_0, the crack growth rate enters Regime 2.

TABLE I
Regressive Coefficients Obtained from the Crack Propagation Paths Derived from Horton's Theory of Bonded Rubber Cylinders with Different Shape Factors

Shape factor S	a_1	a_2	a_3
0.1	−1.4296	2.4619	−1.0323
0.5	−7.2549	12.516	−5.2611
1	−16.739	29.398	−12.66
2.5	−72.835	135.14	−62.303
5	−264.53	507.8	−243.27
7.5	−576.63	1121.3	−544.67
10	−1022.6	2002.4	−979.8
15	−2308.5	4552.6	−2244.1
20	−3935.3	7785.1	−3849.8

TABLE II
Fatigue Parameters of Rubber Compounds EP220, EP330, and EP990 Before and After 6 Months' Thermal Aging Attack[18]

	E (MPa)	c_0 (μm)	G_0 (KJ/m^2)	A	G_t (KJ/m^2)	a	b	G_c (KJ/m^2)
EP220, No aging	19.7	17.25	0.188	0.85	0.61	1.74	3.19	37.4
After 6 months' aging	27.8	11.65	0.239	1.66	0.57	6.37	4.36	28.2
EP330, No aging	25.7	105.71	0.093	0.21	0.35	4.19	4.14	36.3
After 6 months' aging	38.6	38.74	0.113	0.32	0.33	9.47	4.45	29.8
EP990, No aging	18.9	59.52	0.048	0.33	0.39	8.07	4.53	39.6
After 6 months' aging	29.5	11.06	0.150	0.91	0.35	104.62	6.05	28.6

Therefore, the fatigue cycle in the regime can be derived from Eq. (2), which gives as follows:

$$n = \int_{c_{G_0}}^{c_{G_t}} \frac{dc}{A(G(r) - G_0)} = \int_{c_{G_0}}^{c_{G_t}} A^{-1}\left[2\pi(1 + \varepsilon_{P1}(r))^{-1/2} W_C(r)c(r) - G_0\right]^{-1} \times \sqrt{1 + \left(\frac{2a_1 h}{R^2} r + \frac{a_2 h}{R}\right)^2}\, dr. \quad (12)$$

Similarly, c_{G_t} denotes the crack length corresponding to $G = G_t$. Subsequently, the crack growth rate enters Regime 3 when the energy release rate, G, is greater than the transition value, G_t, due to successive crack propagation, leading to a dramatic increase in the crack growth rate. Finally, the fatigue cycle of a bonded rubber cylinder in Regime 3 is derived from Eq. (3) and is found to be:

$$n = \int_{c_{G_t}}^{c_{G_c}} a^{-1}[G(r)]^{-b} dc = \int_{c_{G_t}}^{c_{G_c}} a^{-1}\left[2\pi(1 + \varepsilon_{P1}(r))^{-1/2} W_C(r)c(r)\right]^{-b} \times \sqrt{1 + \left(\frac{2a_1 h}{R^2} r + \frac{a_2 h}{R}\right)^2}\, dr. \quad (13)$$

Accordingly, the fatigue life of circular rubber bearings under cyclic compression can be calculated directly via the above steps. However, the expressions for describing the principal stresses, $\sigma_{P1}(r)$ and $\sigma_{P2}(r)$, the resulting cracking energy density, $W_C(r)$, and the crack length, $c(r)$, along the crack propagation paths are very complicated. As a result, no analytical expressions are possible from the integration in eqs. (12) and (13) Alternatively, a recursive iteration technique is employed. Consequently, the fatigue lives of bonded rubber cylinders under cyclic compression are numerically determined based on various rubber compounds.

RESULTS AND DISCUSSION

The fatigue cycles which correspond to crack propagation in bonded rubber cylinders with a radius of $R = 1$ m and different heights of $h = 5$ m, 0.2 m, and 0.05 m, corresponding to shape factors of $S = 0.1$, 2.5, and 10, respectively, are calculated for different rubber compounds.[18] Moreover, the effects of thermal aging, intrinsic flaw size, and maximum compressive stress are also studied here.

Effect of rubber compound

EPDM rubbers reinforced with three types of carbon blacks N220, N330, and N990, denoted as EP220, EP330, and EP990, are used for the fatigue life prediction of circular rubber bearings. Contents of carbon blacks N220, N330, and N990 for rubber compounds EP220, EP330, and EP990 are 25, 35, and 35 phr, respectively. The Vulcanizing agent of sulfur was utilized here and then cured at 145°C for 4 h for each rubber compound. The fatigue parameters of these three rubber compounds before and after thermal aging attack were measured by Chou, Huang, and Lin,[18] as summarized in Table II. The crack growth rate of rubbers in Regime 1 is assumed to be 5×10^{-4} cm/Mcycle.[13] On the other hand, the fatigue lives are prescribed when a crack grows to a critical length of $c = 0.5$ cm in bonded rubber cylinders; the critical crack length is relatively small when compared with the radius of bonded rubber cylinders, and thus the disturbed stress distribution can be neglected.

Under a maximum compressive stress of 8 MPa, the crack growth rate and fatigue cycle with respect to the crack length in a bonded rubber cylinder with a shape factor $S = 0.1$ are shown in Figure 4(a,b), respectively, including those for the different rubber compounds EP220, EP330, and EP990. In addition, other results for shape factors of 2.5 and 10 are shown in Figures 5 and 6 for comparison. For each rubber compound, it can be seen that the crack growth rate, dc/dn, decreases significantly with the increased shape factor, leading to an improvement in the fatigue resistance of rubber bearings. That is attributed to the reduction of principal tensile stresses and the resulting cracking energy density in bonded rubber cylinders with higher shape factors under compression. Hence, the initial range of energy release rate in Regimes 1 or 2 becomes larger,

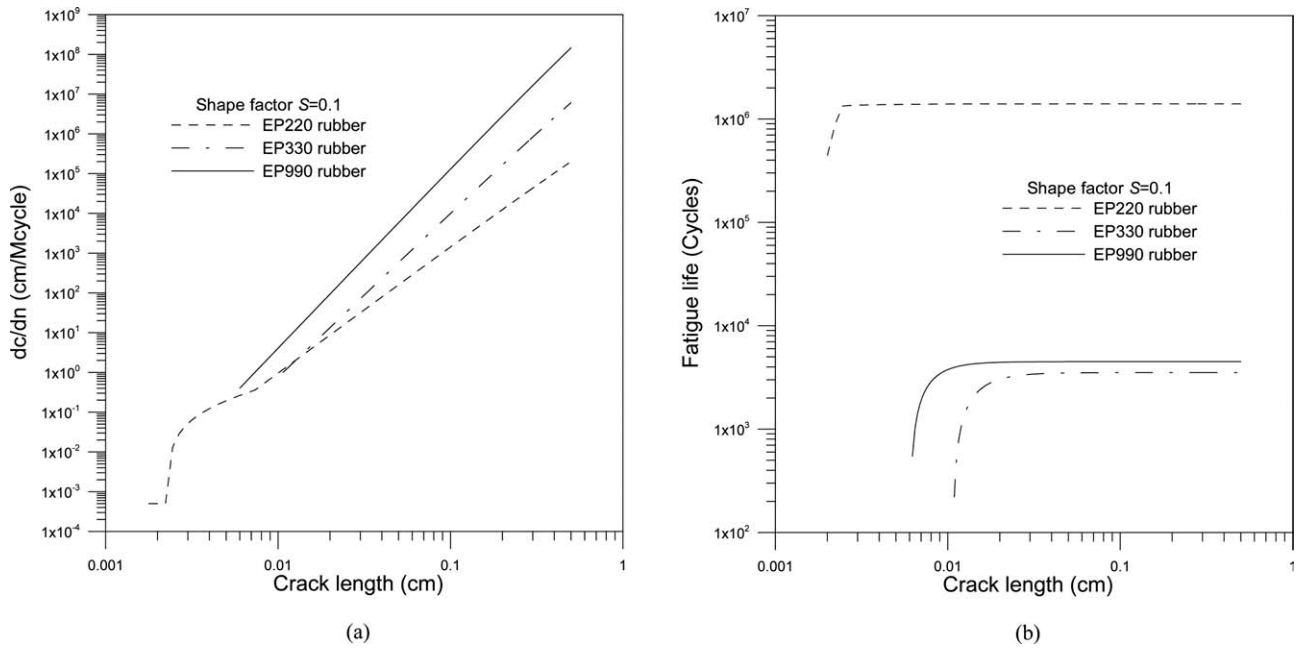

Figure 4 (a) Fatigue crack growth rate and (b) fatigue cycle with respect to the crack length of bonded EP220, EP330, and EP990 rubber cylinders with a shape factor of $S = 0.1$ under 8 MPa cyclic compression.

thus improving the fatigue life of rubber bearings. From Figures 4–6, it is clearly seen that the fatigue cracks in bonded EP220 rubber cylinders all initiate from Regime 1 because of the smallest intrinsic flaw size but the highest threshold value G_0. In other words, they have much better fatigue resistance than other rubber compounds, especially for smaller shape factors. On the other hand, the fatigue resistance of a bonded EP990 cylinder with a shape factor $S = 0.1$ is better than that of EP330, but becomes worse when the shape factor increases to $S = 2.5$ and 10. Indeed, the smaller intrinsic flaw size in rubber compound EP990 enhances the fatigue life of rubber bearings with smaller shape factors. However, for a rubber bearing with a larger shape factor, the energy release rate in Regime 2 is reached earlier

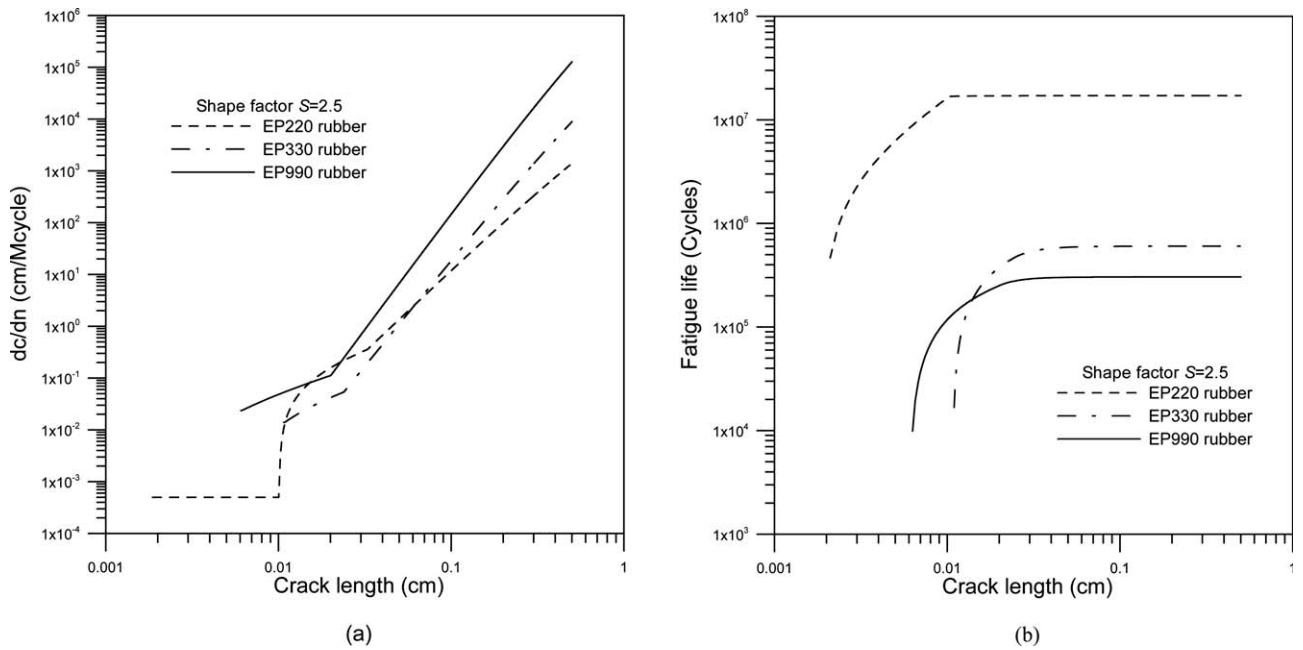

Figure 5 (a) Fatigue crack growth rate and (b) fatigue cycle with respect to the crack length of bonded EP220, EP330, and EP990 rubber cylinders with a shape factor of $S = 2.5$ under 8 MPa cyclic compression.

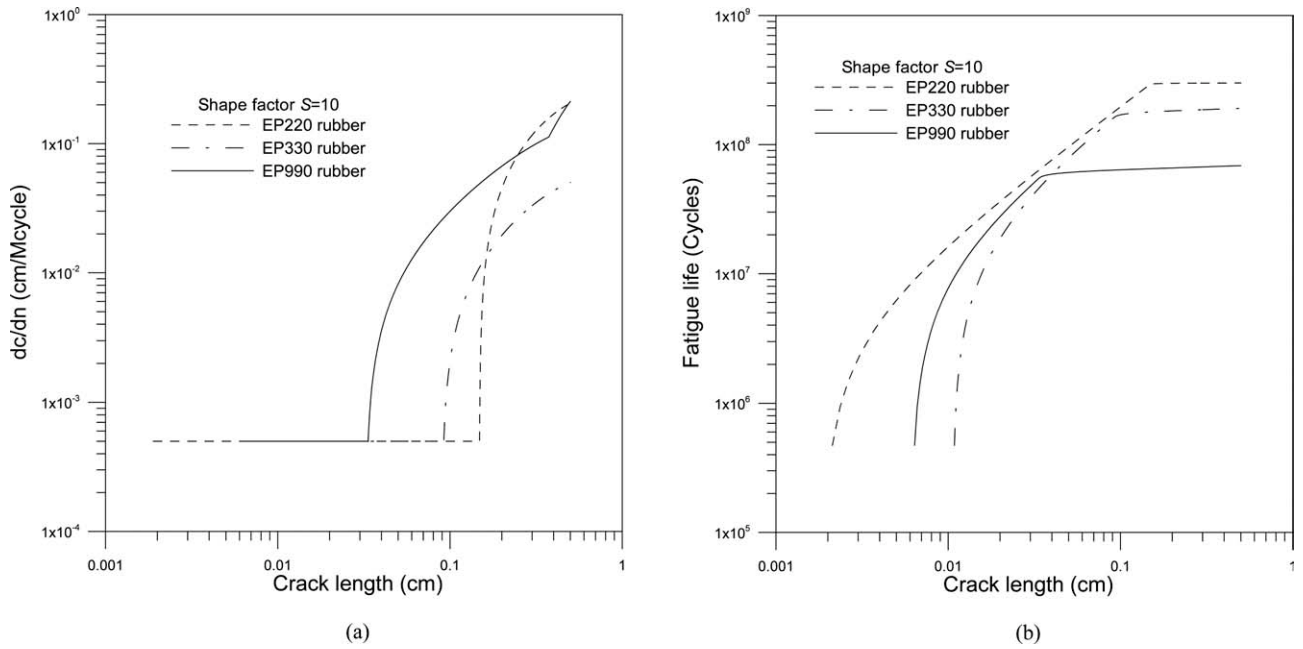

Figure 6 (a) Fatigue crack growth rate and (b) fatigue cycle with respect to the crack length of bonded EP220, EP330, and EP990 rubber cylinders with a shape factor of $S = 10$ under 8 MPa cyclic compression.

due to a lower threshold value, G_0, than for the rubber compound EP330, thus reducing the fatigue resistance. Based on the above findings, it can be said that the intrinsic flaw size, c_0, and the threshold value, G_0, of a rubber compound are the most two important parameters in fatigue life prediction of circular rubber bearings under cyclic compression.

Effect of thermal aging

From Table II, it is found that the intrinsic flaw size c_0 is decreased but the threshold value G_0 is increased after 6 months' thermal aging.[18] To discuss the effect of thermal aging, the results are presented for bonded EP990 rubber cylinders with an extremely small shape factor $S = 0.1$, and another shape factor $S = 10$ commonly designed for practical rubber bearings. Under a maximum compressive stress of 8 MPa, the crack growth rates plotted against the crack lengths in bonded EP990 cylinders before and after 6 months' thermal aging are shown in Figures 7(a) and 8(a) for shape factors of $S = 0.1$ and 10, respectively, and their corresponding fatigue cycles are shown in Figures 7(b) and 8(b). From the figures, it is seen that the fatigue crack initiates from Regime 1 rather than Regime 3 for shape factor $S = 0.1$, and there is an enlarged Regime 1 of crack growth for shape factor $S = 10$ after 6 months' thermal aging. Thus, thermal aging significantly enhances the fatigue resistance of bonded EP990 rubber cylinders. Similar results are also found for rubber compounds EP220 and EP330, and these are attributed to the following reasons. First, the raised Young's modulus due to thermal aging, E, directly reduces the cracking energy density, W_C. Second, the decrease in intrinsic flaw size, c_0, with the increased threshold value, G_0, after thermal aging enlarges the range of Regime 1 of rubber, leading to an improvement in the fatigue resistance of rubber bearings. This occurs even though other fatigue parameters, A, a and b in Regimes 2 and 3 are deteriorated severely due to thermal aging.[18]

Effect of intrinsic flaw size

Assuming rubber compound EP990 with various intrinsic flaw sizes $c_0 = 20$ μm, 40 μm, 60 μm, 80 μm, and 100 μm, the fatigue lives of EP990 rubber bearings corresponding to the shape factors of $S = 0.1$ and 10 under a cyclic compressive stress of 8 MPa are shown in Figure 9(a,b), respectively. From which it is seen that the fatigue resistance of rubber bearings can be enhanced if we reduce the intrinsic flaw size in rubber during manufacture, especially for smaller ones. Rubber bearings made of rubber compound with smaller intrinsic flaws will not only reduce their initial energy release rate but also increase the length of crack propagation required to cause a fatigue failure. For instance, in Regime 1, more than 4×10^6 cycles are enhanced for a reduction of 20 μm of intrinsic flaw size.

Effect of compressive stress

Damage to roads and bridges caused by overloaded vehicles is frequently observed in Taiwan and thus

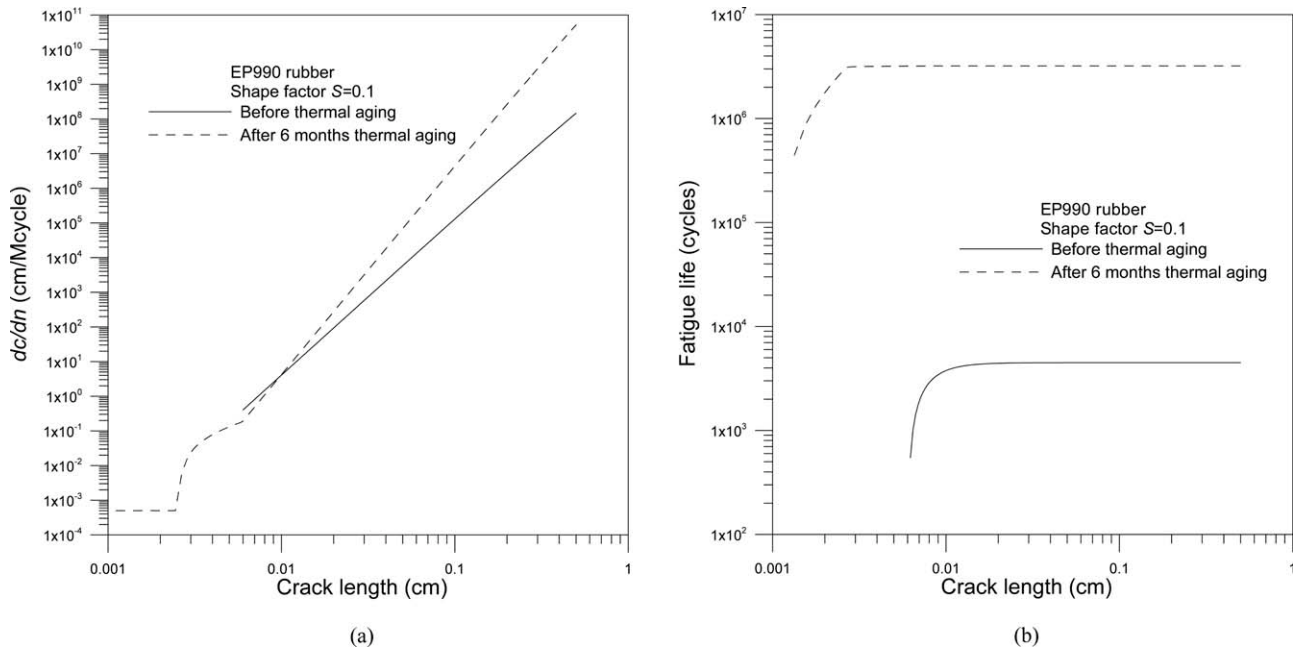

Figure 7 (a) Fatigue crack growth rate and (b) fatigue cycle with respect to the crack length of bonded EP990 rubber cylinders before and after suffering from 6 months' thermal aging with a shape factor of $S = 0.1$ under 8 MPa cyclic compression.

the effect of maximum compressive stress on the fatigue life of rubber bearings is also studied. The fatigue lives of bonded EP990 rubber cylinders under various cyclic compressive stresses are evaluated and plotted in Figure 10(a,b) for shape factors $S = 0.1$ and 10, respectively. It is clearly seen that the fatigue life decreases substantially with increasing compressive stress. Intuitively, this can be attributed to the increase in the resulting cracking energy density, leading to the earlier appearance of Regimes 2 and 3. This reduction in fatigue life is found to be significant; for example, the fatigue life of a bonded EP990 rubber cylinder with a shape factor of $S = 10$ is reduced by one order, from around 6×10^8 cycles

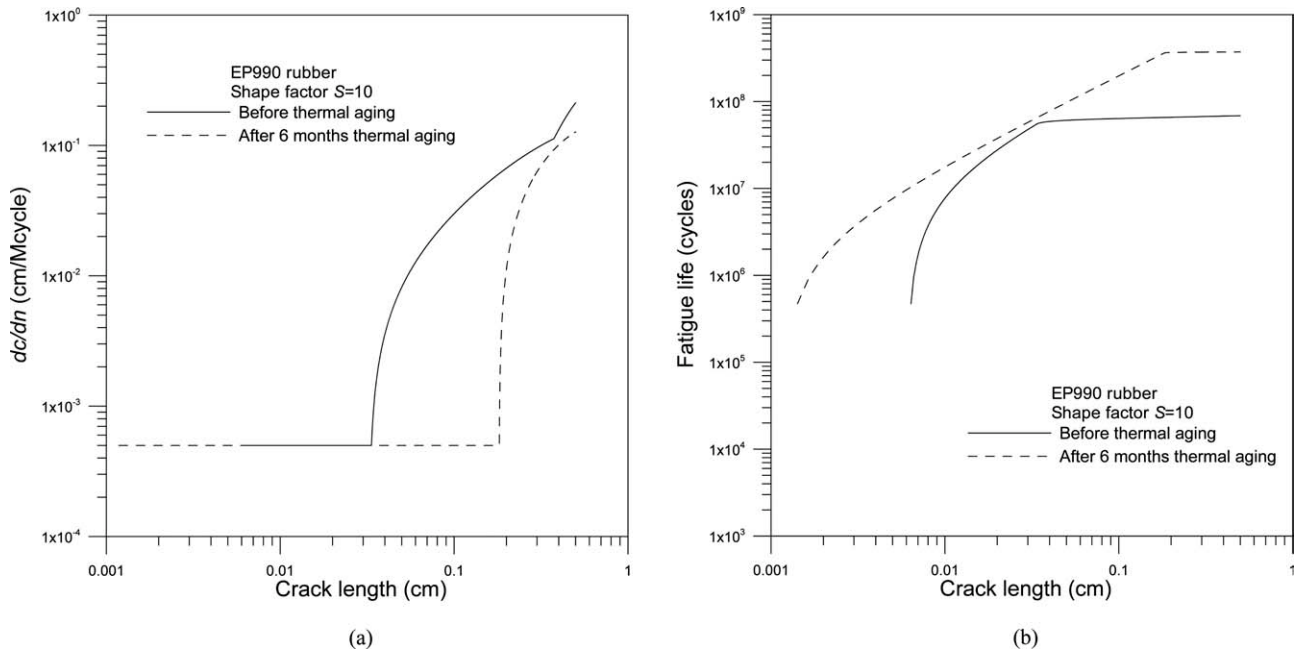

Figure 8 (a) Fatigue crack growth rate and (b) fatigue cycle with respect to the crack length of bonded EP990 rubber cylinders before and after suffering from 6 months' thermal aging with a shape factor of $S = 10$ under 8 MPa cyclic compression.

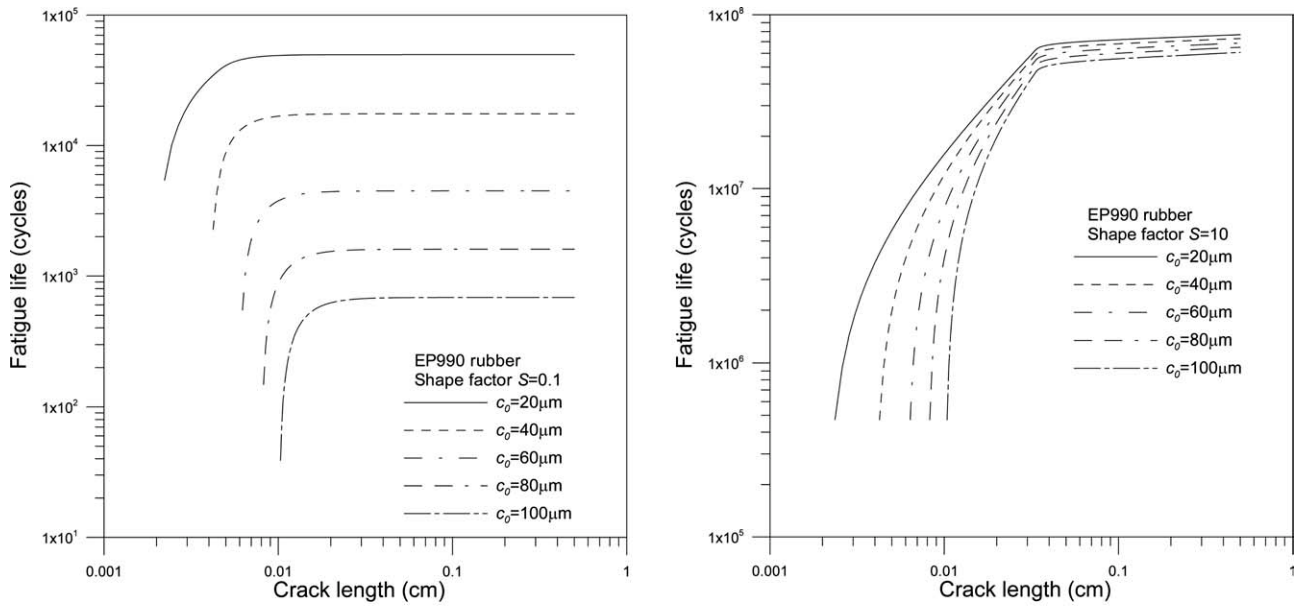

(a) $S = 0.1$ (b) $S = 10$

Figure 9 Effect of intrinsic flaw size on the fatigue life of bonded EP990 rubber cylinders with different shape factors of (a) $S = 0.1$ and (b) $S = 10$.

to around 6×10^7 cycles when the compressive stress is increased from 8 to 16 MPa. Overloads on rubber bearings used in buildings and bridges accelerate the crack propagation in rubber. Consequently, some catastrophic failure of bridges and buildings might occur unexpectedly due to the fatigue failure of rubber bearings caused by overloaded vehicles.

CONCLUSIONS

The fatigue life of circular rubber bearings under cyclic compression is theoretically determined by introducing the cracking energy density and the predicted crack propagation paths. The effects of rubber compounds, thermal aging, intrinsic flaw size, and maximum compressive stress are evaluated. Based

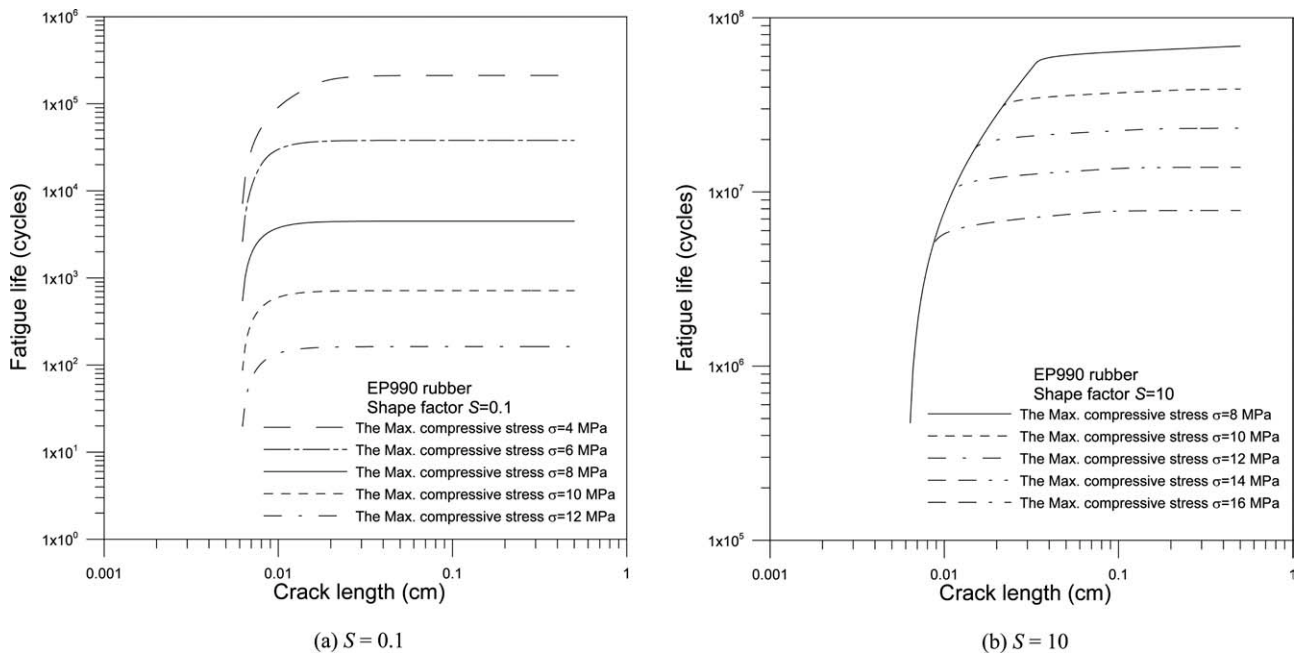

(a) $S = 0.1$ (b) $S = 10$

Figure 10 Effect of maximum compressive stress on the fatigue life of bonded EP990 rubber cylinders with different shape factors of (a) $S = 0.1$ and (b) $S = 10$.

on the above findings, it is concluded that the Regime 1 behavior dominates the fatigue resistance of circular rubber bearings under cyclic compression. In other words, rubber bearings with smaller intrinsic flaw size, c_0, and higher threshold, G_0, have higher fatigue resistance under cyclic compression. As a result, the fatigue resistance of rubber bearings after suffering from thermal aging becomes better, even though the dynamic properties and fatigue parameters in Regimes 2 and 3 are deteriorated severely due to thermal aging. On the other hand, the fatigue life of rubber bearings is decreased substantially by overloading due to the earlier appearance of Regimes 2 and 3 with much higher crack growth rates. A reduction in fatigue life of around one order is found from a doubling of maximum compressive stress. Therefore, the mechanical properties of rubber bearings, their intrinsic flaw size during manufacture, and the maximum cyclic compressive stress in service are of concern and should be taken into account in designing rubber bearings.

References

1. Chou, H. W.; Huang, J. S. J Appl Polym Sci 2008, 107, 1635.
2. Mars, W. V. Tire Sci Technol 2001, 29, 171.
3. Mars, W. V. Rubber Chem Technol 2002, 75, 1.
4. Mars, W. V.; Fatemi, A. Int J Fatigue 2006, 28, 521.
5. Saintier, N.; Cailletaud, G.; Piques, R. Int J Fatigue 2006, 28, 61.
6. Saintier, N.; Cailletaud, G.; Piques, R. Int J Fatigue 2006, 28, 530.
7. Riviln, R. S.; Thomas, A. G. J Polym Sci 1953, 10, 291.
8. Lindley, P. B. J Strain Anal 1972, 7, 132.
9. Lake, G. J.; Lindley, P. B. Rubber Chem Technol 1966, 39, 348.
10. Lake, G. J.; Lindley, P. B. J Appl Polym Sci 1966, 10, 343.
11. Lake, G. J. Rubber Chem Technol 1995, 68, 435.
12. Mars, W. V.; Fatemi, A. Int J Fatigue 2002, 24, 949.
13. Lake, G. J.; Lindley, P. B. J Appl Polym Sci 1965, 9, 2031.
14. Choi, I. S.; Roland, C. M. Rubber Chem Technol 1996, 69, 591.
15. Dizon, E. S.; Hicks, A. E.; Chirco, V. E. Rubber Chem Technol 1974, 47, 231.
16. Hamed, G. R. Rubber Chem Technol 1983, 56, 244.
17. Fielding-Russell, G. S.; Rongone, R. L. Rubber Chem Technol 1983, 56, 838.
18. Chou, H. W.; Huang, J. S.; Lin, S. T. J Appl Polym Sci 2007, 103, 1244.
19. Chou, H. W.; Huang, J. S. J Appl Polym Sci, 2011, 121, 1747.
20. Horton, J. M.; Tupholme, G. E.; Gover, M. J. C. J Appl Mech 2002, 69, 836.
21. Gdoutos, E. E. Fracture Mechanics—An Introduction; Kluwer Academic Publishers: Dordrecht, 1993; Chapter 7.